

Investigating Transport, Mixing and the Formation of Ice in Cumuli with Gaseous Tracer Techniques

JEFFREY L. STITH¹, ANDREW G. DETWILER², ROGER F. REINKING³ and PAUL L. SMITH²

¹*University of North Dakota, Box 8216, University Station, Grand Forks, ND 58202 (U.S.A.)*

²*South Dakota School of Mines and Technology, Rapid City, SD 57701 (U.S.A.)*

³*NOAA/ERL Wave Propagation Laboratory, 325 Broadway, Boulder, CO 80303 (U.S.A.)*

(Received December 12, 1988; accepted March 17, 1989)

ABSTRACT

Stith, J.L., Detwiler, A.G., Reinking, R.F. and Smith, P.L., 1990. Investigating transport, mixing and the formation of ice in cumuli with gaseous tracer techniques. *Atmos. Res.*, 25: 195-216.

Applications of tracer techniques using insoluble sulfur hexafluoride (SF_6) to studies of transport, mixing and the activation of silver iodide (AgI) aerosols in cumuli are presented. One cumulus was treated with SF_6 and the aerosol near the cloud top (-13.5°C), in a region of little vertical transport. Up to 24% of the potential nuclei produced measurable ice particles 7 min after treatment, in accord with the results of recent laboratory measurements of activation of this aerosol by contact nucleation. A second cumulus was treated at the cloud base with SF_6 and the aerosol. The materials were transported to and mixed through the upper regions of the cloud. Ice particles evidently formed near the cloud top (estimated cloud top temperature -13°C). Only low concentrations of natural ice were found in untreated regions of the cloud. In the treated regions the ice particle concentrations in the cold, upper part of the cloud and in downdrafts at lower levels were consistent with the concentrations of AgI nuclei estimated from the tracer measurements. At lower levels of the cloud the materials were not so well mixed, the most concentrated regions being found on the upshear side of the cloud and dilute regions downshear. Mid and upper level ice concentrations were greatest in downdrafts on the downshear side, suggesting that the downdraft was important in transporting the ice to lower levels of the cloud.

RESUME

On applique des techniques de traceur utilisant de l'hexafluorure insoluble de soufre (SF_6) à l'étude du transport, du mélange, et de l'activation des aérosols d'iodure d'argent (AgI) dans les cumulus. Un premier cumulus a été traité avec SF_6 et AgI près de son sommet (-13.5°C), dans une région à faible transport vertical. Jusqu'à 24% des noyaux potentiels ont produit des particules mesurables de glace 7 minutes après le traitement, en accord avec de récentes mesures en laboratoire de l'activité par contact de cet aérosol. Un second cumulus a été traité à sa base avec SF_6 et AgI. Les matières ont été transportées et mélangées dans les parties supérieures du nuage. Manifestement, des particules de glace se sont formées au sommet du nuage (température estimée à -13°C). On n'a trouvé que de faibles concentrations en glace naturelle dans les parties du nuage

non traitées. Dans les parties traitées, les concentrations en particules de glace dans la région surfondue et dans la partie supérieure du nuage, et dans les courants descendants à plus bas niveaux, sont compatibles avec les concentrations en noyaux d'AgI estimées par les mesures du traceur. A des niveaux plus bas du nuage, les matières ont été moins bien mélangées, les parties les plus concentrées étant localisées sur le côté amont des courants ascendants, et les parties les plus diluées sur le côté aval des courants descendants. Les valeurs moyennes et maximales de la concentration en glace sont plus importantes dans les courants descendants sur le côté aval, suggérant que le courant descendant joue un rôle important dans le transport de la glace aux niveaux inférieurs du nuage.

INTRODUCTION

Recently developed fast-response analyzers for insoluble tracer gases, such as sulfur hexafluoride (SF_6), make real-time airborne measurements of tracers possible in small clouds. This provides new high-resolution techniques for the study of cumulus-scale features. Some applications of these techniques to studying transport, mixing and the activation of silver iodide (AgI) aerosols in cumuli are reported here.

This study is part of the North Dakota/NOAA Federal/State Cooperative Program in weather modification research (Reinking, 1985). Objectives of this program relevant to the tracer studies include (1) understanding the transport and dispersion of seeding materials within clouds; (2) investigating the activation of artificial ice nuclei and the growth of the resulting ice particles in relation to natural ice processes in the clouds; and (3) determining the effects of entrainment on the relevant cloud processes. Previous results from this program using the airborne SF_6 tracer techniques are reported in Stith et al. (1986), Stith and Benner (1987) and Stith and Politovich (1989).

Natural trace gases such as ozone or carbon monoxide can be measured with fast-response instrumentation and can be used as tracers (e.g., Dickerson et al., 1987). However, in the troposphere they occur in variable concentrations, which makes them difficult to use as tracers to study cumuli. SF_6 does not occur naturally and background levels (due to anthropogenic releases) are less than 1 part per trillion (ppt). The Benner-Lamb (1985) SF_6 analyzer used in these studies provides relatively low noise (9 ppt) and fast response (less than 1 s), so that low concentrations of SF_6 can be resolved on scales as small as approximately 100 m, with research aircraft flying at 100 m s^{-1} .

Stith et al. (1986) observed that the tracer was transported upward with little mixing in the lower to midcloud regions of various cumuli. Complete mixing across the cloud was observed in the upper cloud regions. These observations are consistent with the measurements of Greenhut et al. (1984), who found the ozone flux due to mean motion in a midlevel cumulus updraft to be two orders of magnitude greater than the turbulent eddy fluxes within the cloud. In another study of isolated nonprecipitating cumuli, Greenhut (1986)

found that mean vertical transport accounted for some 70% of the total cloud flux of ozone, whereas cloud turbulence contributed only 30%.

Case studies of the mixing process in the upper regions of cumuli are described in Stith and Benner (1987) and Stith and Politovich (1989). In the latter study the SF₆ tracer was used to investigate the effects of cloud-top mixing on the droplet size spectra in a small cumulus. Their observations suggested that this mixing may provide a cloud-top source of small droplets which could help explain the bimodal nature of some cloud droplet size spectra.

Previous tracer investigations of ice formation in cumuli demonstrated the utility of releasing and tracking SF₆ mixed with AgI aerosols in supercooled clouds. This technique was used to separate the effects of the AgI from natural ice formation (Stith et al., 1986) and to investigate the evolution of the ice particles produced by the AgI seeding (Stith and Benner, 1987).

In this paper two methods of experimentation using SF₆ and AgI aerosol are illustrated by two case studies of individual cumuli. The first method examines a treated cumulus within a narrow temperature zone to determine the history of ice formation by the AgI aerosol, in such a way that the nucleation can be compared with predictions from previous laboratory studies in an isothermal cloud chamber. This requires treating a cloud region where vertical transport is minimal (e.g., near the top of a cloud showing little vertical growth). The second method examines the treated region after significant vertical transport, allowing ice formation by the AgI through a range of temperatures and mixing regions in the cloud. Treatment at the cloud base was used to replicate a standard cloud seeding practice, so this method examines the effects of ice nuclei that originate at the cloud base.

INSTRUMENTATION AND METHODOLOGY

In the present work, airborne releases of gaseous SF₆ along with AgI-AgCl aerosols from acetone burners were performed on 22 and 28 June, 1987, near Dickinson, ND. Release rates of SF₆ were 0.5 and 0.3 kg km⁻¹ for 22 June and 28 June, respectively. An acetone solution containing AgI and other salts was burned to yield an AgI release rate of 0.5 g km⁻¹.

In addition to a release aircraft, the University of North Dakota Cessna Citation and the South Dakota School of Mines T-28 research aircraft were used for sampling. The Citation carried Particle Measuring Systems (PMS) probes (FSSP, 2DC, and 1DP) for measuring cloud and precipitation particle size spectra, a Johnson-Williams (JW) sensor for cloud liquid water, an Inertial Navigation/Gust Probe (INGP) system for wind measurements, an NCAR-type reverse-flow cloud temperature sensor, a Cambridge Systems dew-point hygrometer, pressure transducers for measurement of static and pitot pressures and the SF₆ analyzer. The FSSP data were corrected for droplet

sizing and concentration errors due to optical coincidence and electronic dead time losses as described by Baumgardner et al. (1985).

The instrumentation on the T-28 (Johnson and Smith, 1980) included PMS FSSP and 2DC probes, similar pressure and temperature sensors, and an essentially identical SF₆ analyzer. However, the analyzer on the T-28 was operating in an unheated, unpressurized cockpit and showed a much lower signal-to-noise ratio than the Citation instrument. The latter could discriminate concentrations less than 10 ppt without any postprocessing of the data, while concentrations less than 100 ppt could not be reliably measured by the T-28 unit even after filtering the data. The FSSP data from both aircraft were processed in a similar manner, although the T-28 instrument is older and data on the electronic dead time are not recorded directly but rather estimated from the measured droplet concentrations.

The aircraft coordinated visually and by radio communication. Further guidance came from a meteorologist on the ground with access to quantitative weather radar and air traffic control radar flight track information. Postanalysis of aircraft "skin paint" echoes in the weather radar data showed the aircraft operations to be well coordinated.

A real-time software "pointer" system based on the INGP system was used to assist in guiding the Citation back to the tracer region once the pointer system was initialized upon first detecting the tracer. The system displays heading, distance, elapsed time and altitude required to intercept a parcel of air assumed to be moving with the measured wind field. The horizontal portion of the pointer system proved to be quite helpful in repeatedly locating cloudy regions tagged with SF₆, particularly in smaller clouds, but eventually it diverged from the tagged region. These errors were minimized by updating the pointer on each successive plume interception. The SF₆ data from the T-28 were telemetered to the meteorologist at the ground for use in directing its operations. Sampling was conducted along the horizontal windshear axis (when possible) to increase the chances of hitting the tracer plume as it drifted toward the downshear side of the cloud.

Measurements made after SF₆ releases directly into ice-free supercooled clouds at temperature levels warmer than -7°C (the approximate activation point of the AgI aerosol) have not revealed any formation of ice (e.g., Stith et al., 1986). This suggests that neither the SF₆ release method nor the treatment aircraft itself produced ice particles (e.g., as suggested by Rangno and Hobbs, 1984), at least at these relatively high temperatures. Further tests, using SF₆ only, are planned to confirm these results over a broader range of temperatures. This was not a concern for the 28 June case, where the cloud base releases were made at $+6^{\circ}\text{C}$.

It is assumed that, during typical sampling periods (20 min), the AgI aerosols disperse with the SF₆ until nucleation scavenging removes the particles. Within these periods any ice particles produced by the aerosol should become

detectable by PMS 2DC probes. The 2DC probes were used as the primary detectors for ice particles; the probes on the Citation and the T-28 have resolutions of $33 \mu\text{m}$ and about $30 \mu\text{m}$, respectively. Until the particles become large enough that their shapes can be inferred from the 2DC data (i.e., larger than about $100 \mu\text{m}$), it is not possible to distinguish ice from water. We assume the small particles to be ice if subsequent passes through the same region reveal the development of only ice particles in the particles whose shapes are discernible.

The nucleation characteristics of the AgI-AgCl aerosol used in this study are discussed by DeMott et al. (1983). The primary freezing mechanism is thought to be contact nucleation. Consequently, the rate of ice formation is affected not only by the concentrations of the AgI aerosol, but also by the cloud characteristics such as cloud droplet and liquid water concentrations.

Following Stith and Benner (1987), we estimate the fraction, F , of nuclei activated and grown to detectable sizes by:

$$F = \frac{Q_t C_i}{E Q_a C_t} \quad (1)$$

Here Q_t and Q_a are the release rates of tracer and AgI, respectively, and C_i and C_t are the measured concentrations of ice particles and tracer, respectively. E is the total ice crystal production effectiveness (in crystals per gram of AgI), which was determined from isothermal cloud chamber tests on AgI-AgCl aerosols at Colorado State University.

Eq. (1) can be used in several ways. In Stith et al. (1986) it was used to estimate the maximum ice particle concentration that could have been formed through primary production of ice by the AgI aerosol (i.e., $F=1$) on the basis of the measured tracer concentrations. This was compared with the measured ice particle concentrations in treated clouds to determine if the observed ice could have been due solely to the AgI aerosol. In Stith and Benner (1987) F was determined as a function of time for a treated cloud that slowly developed small ice crystals. Here we compare the history of F in the 22 June cloud with the laboratory results of DeMott et al. (1983), who describe the number of nuclei activated as a function of time in their isothermal cloud chamber for various liquid water concentrations and temperatures.

OBSERVATIONS OF ICE ACTIVATION, TRANSPORT AND MIXING

Ice activation over a time interval

On 22 June, the upper region of a small and not very active cumulus congestus cloud was treated by a single pass at -11.5°C . The cloud base temperature was not measured, but clouds in the area had bases as warm as $+11^\circ\text{C}$. The measurements obtained during four sampling passes by the Citation at -13.5°C

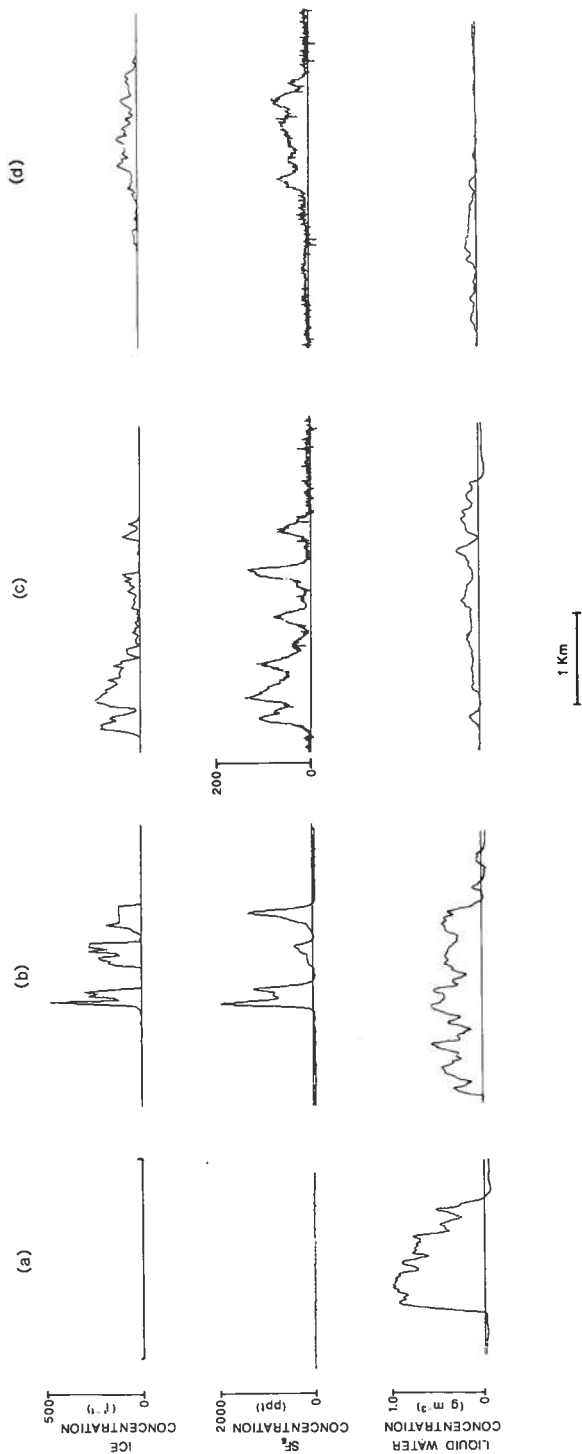


Fig. 1. Concentrations of ice particles (from 2DC shadow-or), SF₆ and cloud liquid water (from JW) observed by the Citation on 22 June, 1987, 300 m above treatment altitude (at a temperature of -13.5°C) at: (a) the time of treatment; (b) 4 min after treatment; (c) 7 min after treatment; and (d) 10.5 min after treatment.

(300 m above the treatment altitude) are shown in Fig. 1. The cloud was free of ice (Fig. 1a) at the time of treatment. On the second sampling pass (Fig. 1b) small ice particles developed in three regions which together comprised about half of the cloud width. The boundaries and variations of these regions correlated well with those of the tracer regions; this is rather convincing evidence that the ice was formed by the AgI treatment and did not develop naturally in the cloud. However, the amounts of ice observed per unit amount of tracer varied somewhat from region to region; this may be a result of slightly different nucleation and growth conditions present in these regions during the 4 min between treatment and sampling.

On the third pass, some 7 min after treatment (Fig. 1c), the ice, SF₆ and liquid water were well mixed throughout the cloud top; as before, the amounts of ice per unit amount of SF₆ in the cloud varied with location. The SF₆ levels were diluted by almost an order of magnitude, while the ice concentrations were similar to the previous pass. This suggests that the amount of ice increased appreciably between passes 2 and 3. On the final pass, 10.5 min after treatment, the spatial distributions of ice and water (Fig. 1d) resembled those found during the third pass.

The growth of the ice particles and the depletion of the cloud droplet mode are clearly evident in the evolution of the particle size spectra during passes 2, 3 and 4 (Fig. 2). The PMS 2DC imagery reveals that during the second pass (Fig. 3, top) the cloud contained irregular ice particles ranging from a few pixels in size to almost 500 μm . Growth to millimeter sizes was observed during passes 3 and 4 (Figs. 2, 3). Irregular ice particles mixed with stellar or sector plate crystals were observed (Fig. 3). The presence of the latter particles, which form at temperatures near that of the sampling altitude (or slightly colder), suggests that the ice particles were formed near the treatment altitude and were not carried up from lower cloud regions.

Table I compares the estimated cumulative fraction of ice nuclei activated and grown to detectable sizes from eq. (1) with the results in fig. 6 of DeMott et al. (1983). Their results for chamber conditions of 0.5 g m⁻³ liquid water and -12°C were used in Table I. Peak values of the observed ice particle and tracer concentrations were used in eq. 1 for each of the regions indicated. These were chosen because they are most likely to be representative of the more ideal constant growth conditions present in the chamber. Four minutes after treatment (pass 2) the observed activation fraction varied from 1.4% to 6.3%; the latter value represents about half of that observed in the cloud chamber results (Table I). Given that a substantial number of ice particles near the 2DC detection threshold (33 μm) were observed (Figs. 2 and 3), it is likely that a significant fraction of the ice particles that had been nucleated had not yet grown to detectable sizes. At 7 min after treatment (pass 3) the observed fraction (24%) nearly matched the cloud chamber results (22%), while at 10.5

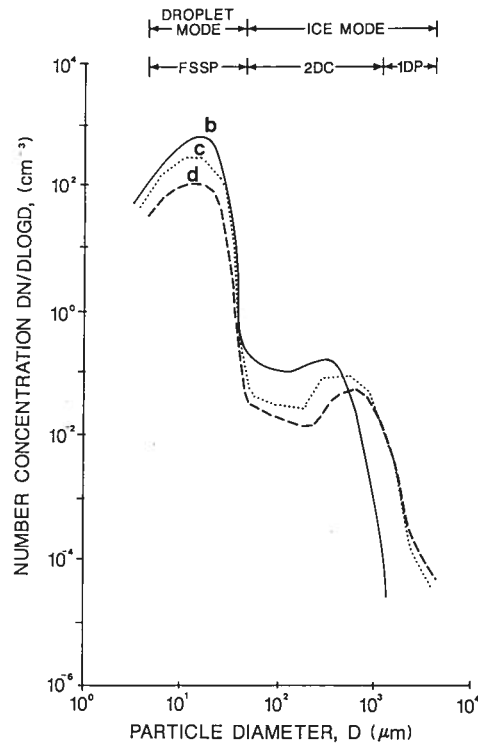


Fig. 2. Average particle size distributions for the regions (b)–(d) in Fig. 1.

min (pass 4) it decreased to about 15% versus 33% expected from the cloud chamber results.

Both the cloud chamber results and F measured in the cloud suggest that less than a third of the available AgI nuclei had produced ice particles in 10.5 min. Continued activation and growth of the remaining nuclei might have served as a source for the continual development of small ice particles. This was not observed, as the concentration of small ice particles (33–300 μm) decreased monotonically with time (Fig. 2). Since these nuclei are expected to act through contact nucleation, the observed rapid decline of the cloud droplets and liquid water (Figs. 1 and 2) suggests that the rate of nucleation dropped off rapidly due to the decrease in the number of cloud droplets available to drive the contact nucleation process. Thus, the total ice production was probably limited more by the availability of cloud droplets than by the number of available ice nuclei. This would also help explain the discrepancy between the cloud chamber results at a constant 0.5 g m^{-3} of liquid water and the measured value of F during pass 4.

The observation that F actually decreased slightly (rather than remaining constant) between passes 3 and 4 suggests that the effects of particle fallout

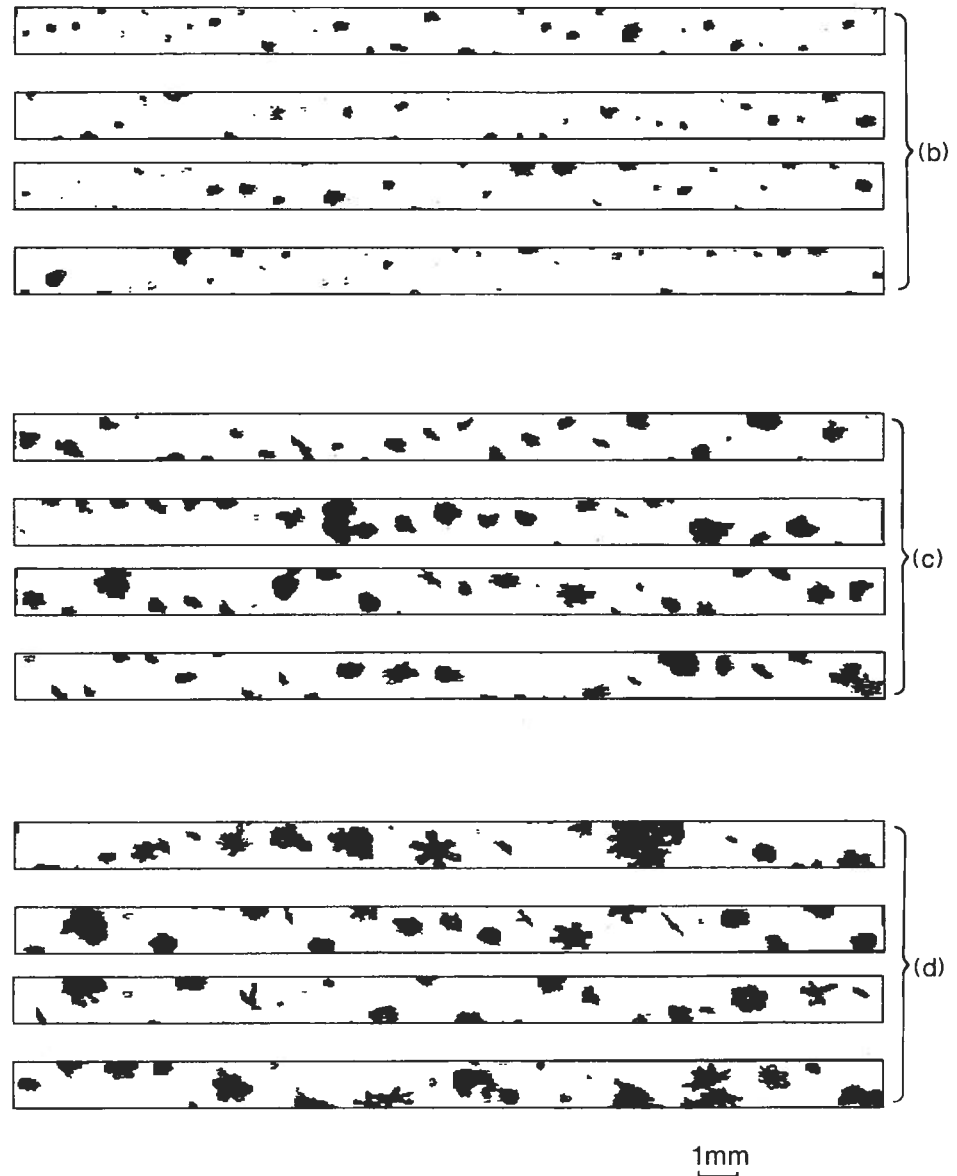


Fig. 3. Examples of particle images from the PMS 2DC probe for each of the regions (b)-(d) in Fig. 1.

and aggregation were evident. This is not surprising, given the large sizes of many of the observed particles 7 to 10.5 min after treatment. Some aggregation is also evident in the particle images (Fig. 3), although relatively pristine crystals were also present.

TABLE I

Cumulative fraction of ice nuclei activated

| | Pass 2 | | | Pass 3 | Pass 4 |
|-----------------------------------|--------------|---------------|--------------|--------|--------|
| | first region | middle region | third region | | |
| Time from treatment (min) | 4 | 4 | 4 | 7 | 10.5 |
| F from eq. 1 (%) | 2.2 | 6.3 | 1.4 | 24 | 15 |
| Activation fraction* ¹ | 12 | 12 | 12 | 22 | 33 |

*¹DeMott et al. (1983).*Vertical transport, mixing and ice activation from cloud-base releases**Transport and dispersion*

On 28 June a cumulus cloud of similar size was treated for 15 min beginning at 1620 MDT (hereafter designated t_0) by a continuous release during orbits at 2.5 km MSL (and 5.8°C), near the cloud base. (However, the acetone burner initially selected malfunctioned, so the AgI release actually began about 2 min later than t_0 .) At t_0 the maximum updraft speed at the release level was about 2.5 m s⁻¹. Initial cloud penetrations 0.5 km (T-28) and 1.5 km (Citation) above the cloud base showed temperatures of 2°C and -5°C, and maximum cloud liquid water concentrations (LWC) of 0.6 g m⁻³ and 1.0 g m⁻³, respectively. Neither aircraft encountered any ice particles and there was no radar echo at that time.

The two aircraft then executed a series of coordinated penetrations, maintaining a separation of about 1 km in altitude and ascending gradually higher in the cloud over the next 35 minutes. The sampling passes were made along the horizontal wind shear axis. Data from these passes are presented in Figs. 4-9, so that left to right corresponds to upshear and downshear (i.e., not as a time series). The estimated cloud top height and temperature were 5.5 km MSL and -13°C, respectively, with little vertical development during the period of observations.

During the passes at t_0 and about $t_0 + 4$ min, neither aircraft detected any SF₆. The T-28 first encountered a high concentration of SF₆ (greater than its detection limit of 100 ppt) 0.7 km above the release level at $t_0 + 8$ min. At the Citation level SF₆ was first found 1.5 km above the release level at $t_0 + 11$ min. Fig. 4, representing cloud LWC and SF₆ data from three successive coordinated penetrations, shows that the plumes detected at the T-28 levels were no more than 1 km wide. Therefore a plume may have been missed at the T-28 level on the $t_0 + 4$ penetration. At the Citation levels, however, the SF₆ had spread across the active region of the cloud; thus one can take the appearance of the tracer 1.5 km above the release level between the $t_0 + 8$ and $t_0 + 11$ min passes

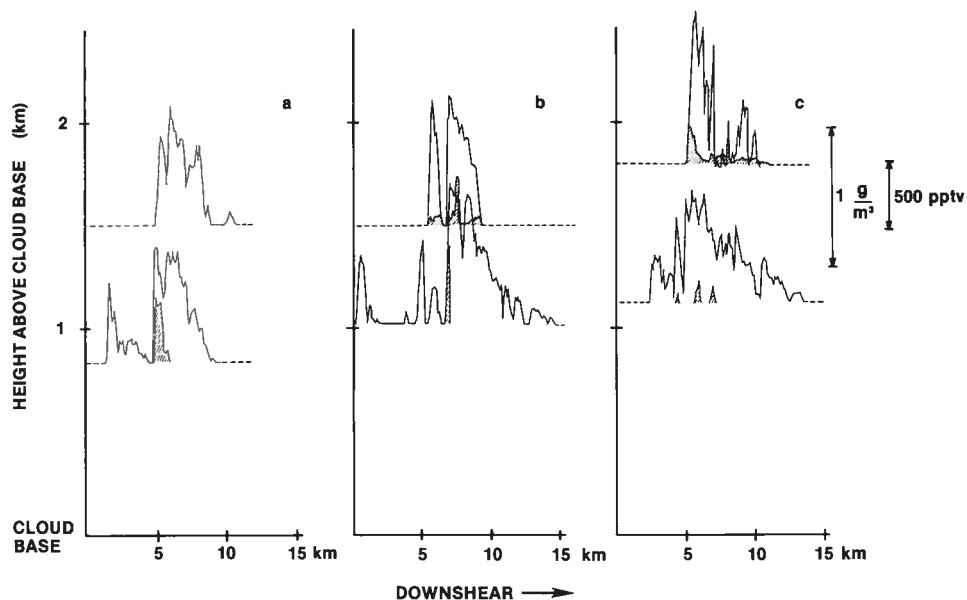


Fig. 4. Plots of cloud liquid water concentration (solid line, unfilled) and SF_6 volume mixing ratio (solid line, filled) from the Citation (upper) and T-28 (lower) data on 28 June 1987, shown in cloud-relative spatial coordinates. The data are from penetrations at (a) 8 min, (b) 11 min, and (c) 16 min following the beginning of the release near cloud base. Citation LWC values are taken from its J-W sensor, while T-28 data are from its FSSP.

as an indication of the transport time. This suggests an average vertical transport speed of about 2.5 m s^{-1} in the lower half of this cloud.

During the $t_0 + 8$ min penetration (Fig. 4a) the T-28 encountered a narrow plume of SF_6 with a peak concentration of about 500 ppt on the upshear edge of the stronger cell. No vertical wind data are available from the T-28 on this flight, but FSSP cloud droplet spectra inside this plume were very narrow and indicative of relatively unmixed, ascending cloud base air. Peak LWC values were approximately equal to adiabatic values estimated from the cloud base properties.

On the following penetration at $t_0 + 11$ min (Fig. 4b) the lower aircraft (T-28) again detected a narrow tracer plume, 1.0 km above the release level, with a peak concentration of 500 ppt on the upshear side of the main cell. Regions of low SF_6 concentration, if present, would not have been detected with the T-28, so some of these regions could also have been present. The Citation, 0.5 km higher up, found low concentrations of SF_6 distributed across the updraft region of the cloud, with one narrow peak in the middle of the main cell reaching a concentration of 350 ppt.

On the next coordinated penetration (Fig. 4c) at $t_0 + 16$ min, corresponding to the end of the cloud-base release period, the T-28 encountered three narrow

plumes 1.2 km above the release level. Each plume corresponded to a local maximum in the cloud LWC at this level. The upper aircraft, 1.8 km above the release level and about 1 km below cloud top, found low concentrations of the tracer throughout the cloud, with a narrow region of much higher concentration on the upshear side.

The two aircraft continued to penetrate the cloud for another 20 min, eventually climbing to 1.7 and 2.7 km, respectively, above the release level. The T-28 encountered no more regions where the SF_6 concentration exceeded 100 ppt. The Citation continued to find low concentrations of the tracer well mixed through the upper regions of the cloud, with somewhat higher concentrations on the upshear side.

The picture that emerges from these observations is one of transport in nar-

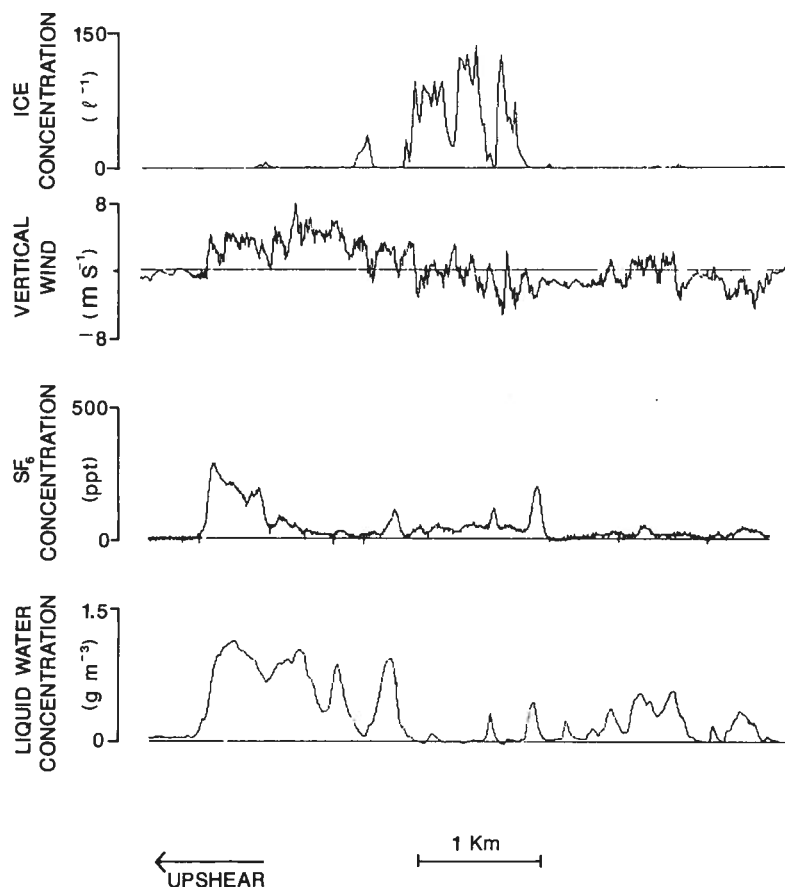


Fig. 5. Vertical wind and the concentrations of ice particles, SF_6 and cloud liquid water at cloud midlevels (-7°C , 1.8 km above the release level) from the Citation data on the $t_0 + 16$ min penetration on 28 June, 1987.

row plumes up through the lower 1 km or more of cloud, on the upshear side, followed by dispersion across the upper part of the cloud. This resembles findings from the earlier tracer experiments (e.g., Stith et al., 1986) but the coordinated aircraft penetrations at different levels in the cloud provide a more complete picture of the plume evolution.

Mixing and ice activation

Both aircraft encountered only a few ($< 1 \text{ l}^{-1}$) small ($< 100 \mu\text{m}$) ice particles during the $t_0 + 11$ min penetration, in an untreated cloud region at the LWC null at about $x=6$ km in Fig. 4b. This was the first observation of any ice in the cloud. The Citation vertical wind data, at the -4°C level, showed a well-organized downdraft with a peak speed of -5 m s^{-1} in this region, indicating that these particles came from higher in the cloud. These low concen-

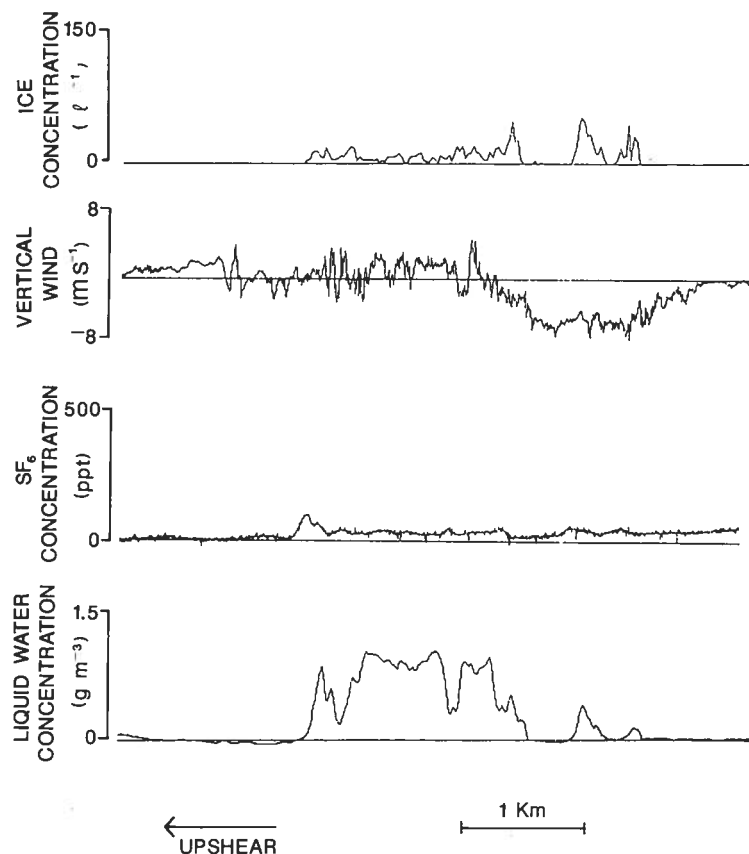


Fig. 6. As in Fig. 5, except at -10°C , 2.4 km above the release level, on the $t_0 + 19$ min penetration.

trations of natural ice, along with significant cloud LWC and updrafts on the upshear side, made this an ideal candidate for AgI cloud seeding.

The Citation observed the first significant amount of ice in a portion of the treated region on the $t_0 + 16$ min penetration at the -7°C level (1.8 km above the release level). (During the sampling passes the in-cloud temperature was within approximately $\pm 0.6^\circ\text{C}$ of the value stated for the pass. This indicates that the cloud was near buoyant equilibrium, at least at these mid to upper levels.) Small ice particles were observed in concentrations up to nearly 150 l^{-1} on the downshear side of the cloud in downdraft (Fig. 5). Relatively concentrated tracer was found mixed through about half the updraft on the upshear side in ice-free regions; more dilute tracer was found downshear in the downdraft region that contained the ice particles (Fig. 4c and 5). The T-28 observed no ice particles on this pass 0.8 km lower down.

On passes at $t_0 + 19$ and $t_0 + 21$ min (both made at -10°C , 2.4 km above the release level), the Citation found ice particles and tracer mixed through

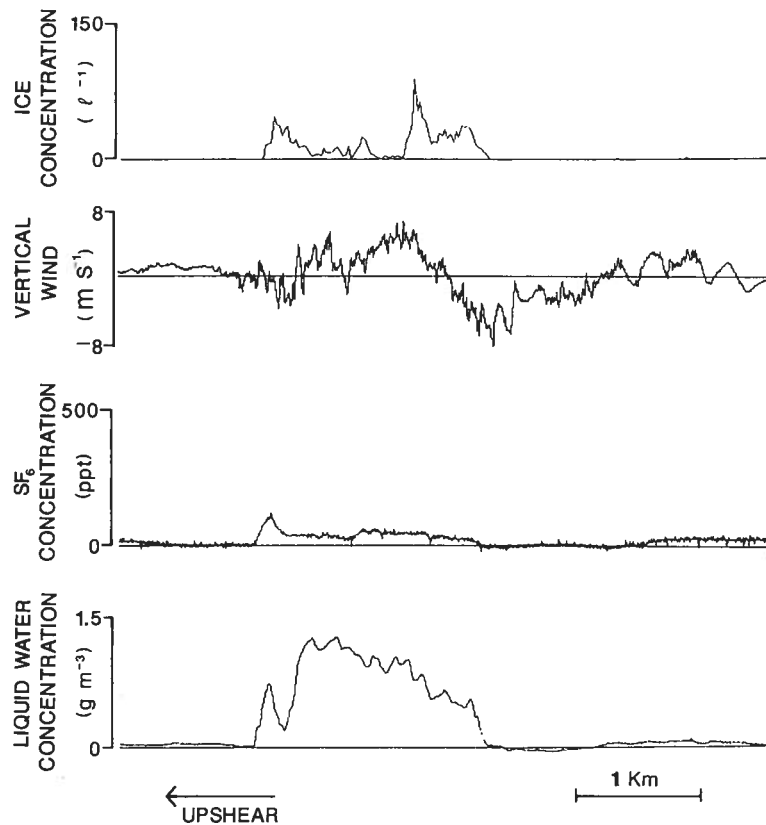


Fig. 7. As in Fig. 5, except at -10°C , 2.4 km above the release level, on the $t_0 + 21$ min penetration.

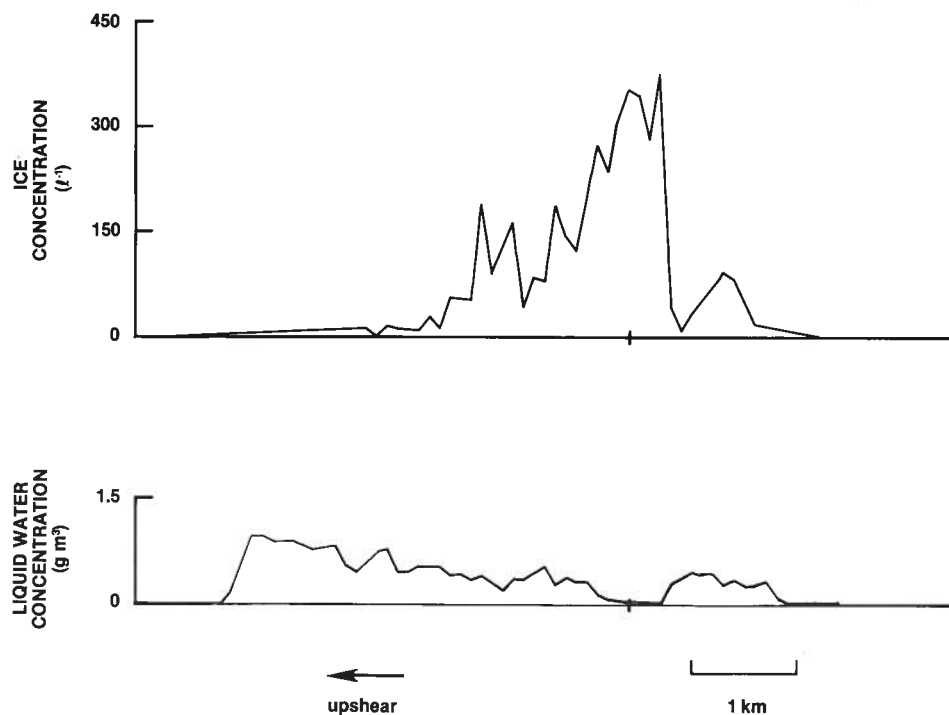


Fig. 8. Concentrations of ice particles and cloud liquid water from the T-28 data at the -4°C level (1.3 km above the release level) on the $t_0 + 21$ min penetration on 28 June 1987. The T-28 found no detectable SF_6 (i.e. greater than 100 ppt) on this penetration.

most of the cloud (Figs. 6 and 7). As observed on the preceding pass, the highest tracer concentrations were found on the upshear side. At $t_0 + 19$ (Fig. 6) the highest ice concentrations were found on the downshear side, in downdraft; at $t_0 + 21$ (Fig. 7) more ice appeared in the updraft regions. The T-28 also observed ice particles on the $t_0 + 21$ penetration (Fig. 8) at the -4°C level, 1.3 km above the release level.

At $t_0 + 23$ min the Citation made a pass at -11°C , 2.5 km above the release level and very near the cloud top (Fig. 9). Both ice particles and tracer were spread through the (weak) updraft region, and the upshear/downshear distinction was not as pronounced as the earlier passes. This region contained some of the highest liquid water concentrations of any of the passes, indicating that the cloud remained active, with supercooled water near the top, 25 min into the case.

The particle size distributions and 2DC images for each of the Citation passes are presented in Figs. 10 and 11, respectively. The size distributions evolved in a manner similar to that indicated in Fig. 2, except that the droplet mode remained relatively constant. However, the images clearly show the particles

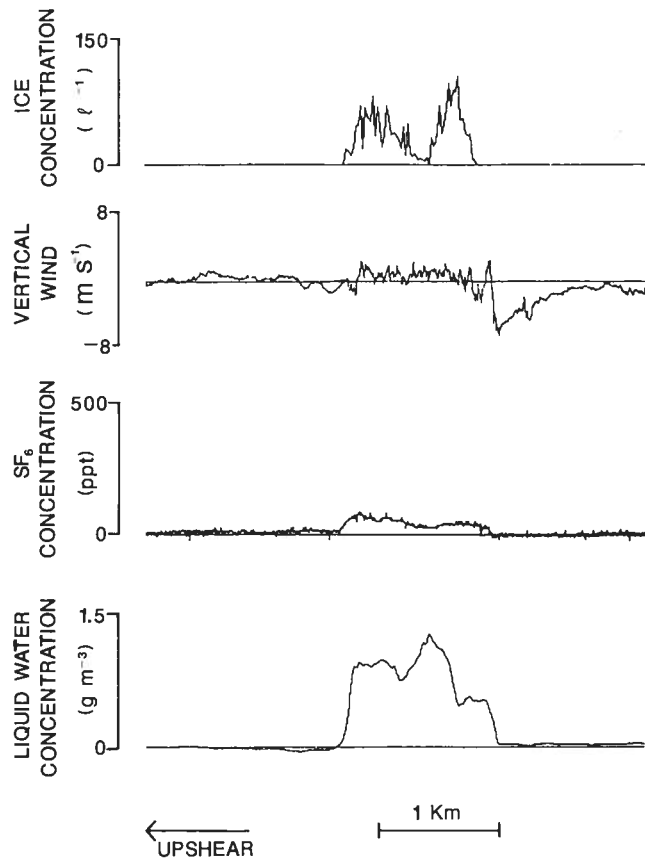


Fig. 9. As in Fig. 5, except near the cloud top (-11°C , 2.5 km above the release level) on the $t_0 + 23$ min penetration.

developing as graupel in this cloud which maintained significant supercooled cloud liquid in its upper levels for a much longer time. The particles observed by the T-28 on the $t_0 + 21$ min penetration 1.1 km below the Citation were similar to, but somewhat larger than, those shown in Fig. 11c.

The ice particle concentrations observed in the downdraft region at -7°C (Fig. 5) were up to two orders of magnitude greater than the maximum ($F=1$) that would be predicted by eq. 1, due to the low value of E at this temperature. This suggests that the particles initially developed higher up in the cloud.

For the -10°C level, setting $F=1$ in eq. 1 predicts a maximum ice particle concentration of 380 l^{-1} for an SF_6 concentration of 100 ppt. Thus the ice concentrations observed at the -10°C level (Figs. 6,7) were somewhat less than the maximum which would have resulted from the primary production of ice by the AgI aerosol at that temperature. The nucleation of ice on the aerosol is a rate process and the elapsed time since the materials passed above the

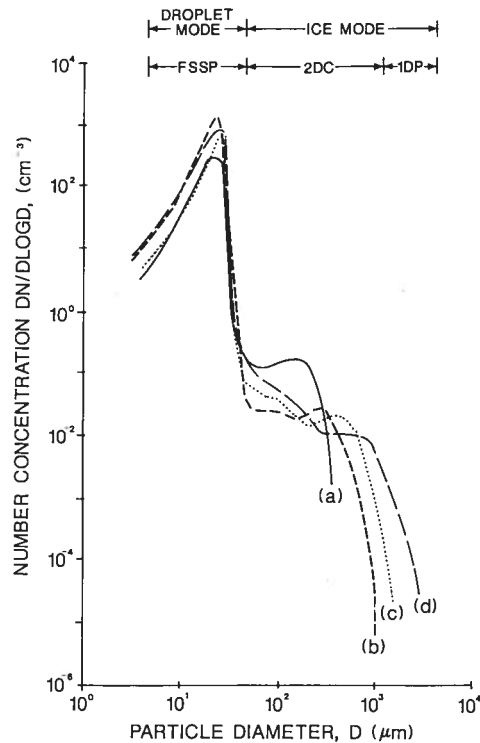


Fig. 10. Average particle size distributions for the ice particle regions in Figs. 5, 6, 7 and 9. These are labeled (a)–(d), respectively.

–4°C level was at least 8 min. Consequently there was adequate time for activation of some but not all of the nuclei and growth to the observed particle sizes (Fig. 11b,c). In some cases those sizes were large enough that sedimentation could be separating the particles from the initial tracer regions. Growth and fallout would continually remove particles, but not the SF₆ tracer, from the cloud top region. As a result, and considering the activation time of the agent as observed on 22 June and in the cloud chamber, it is not surprising to find $F < 1$ in this situation. Thus the observed particle concentrations are consistent with a mechanism of ice production by the AgI nuclei. Since the tracer and AgI were transported vertically over a range of temperatures, this cloud would not be likely to produce the same correlations between ice particles and tracer concentrations as were observed in the 22 June experiment. This makes it more difficult to establish a definite association between ice production in the cloud and the AgI agent.

The cloud developed an initial radar echo (15 dBz) at about 4.7 km MSL and about $t_0 + 22$ min (Fig. 12). This was near the Citation penetration altitude at that time and indicates a first-echo temperature of about –9°C. This

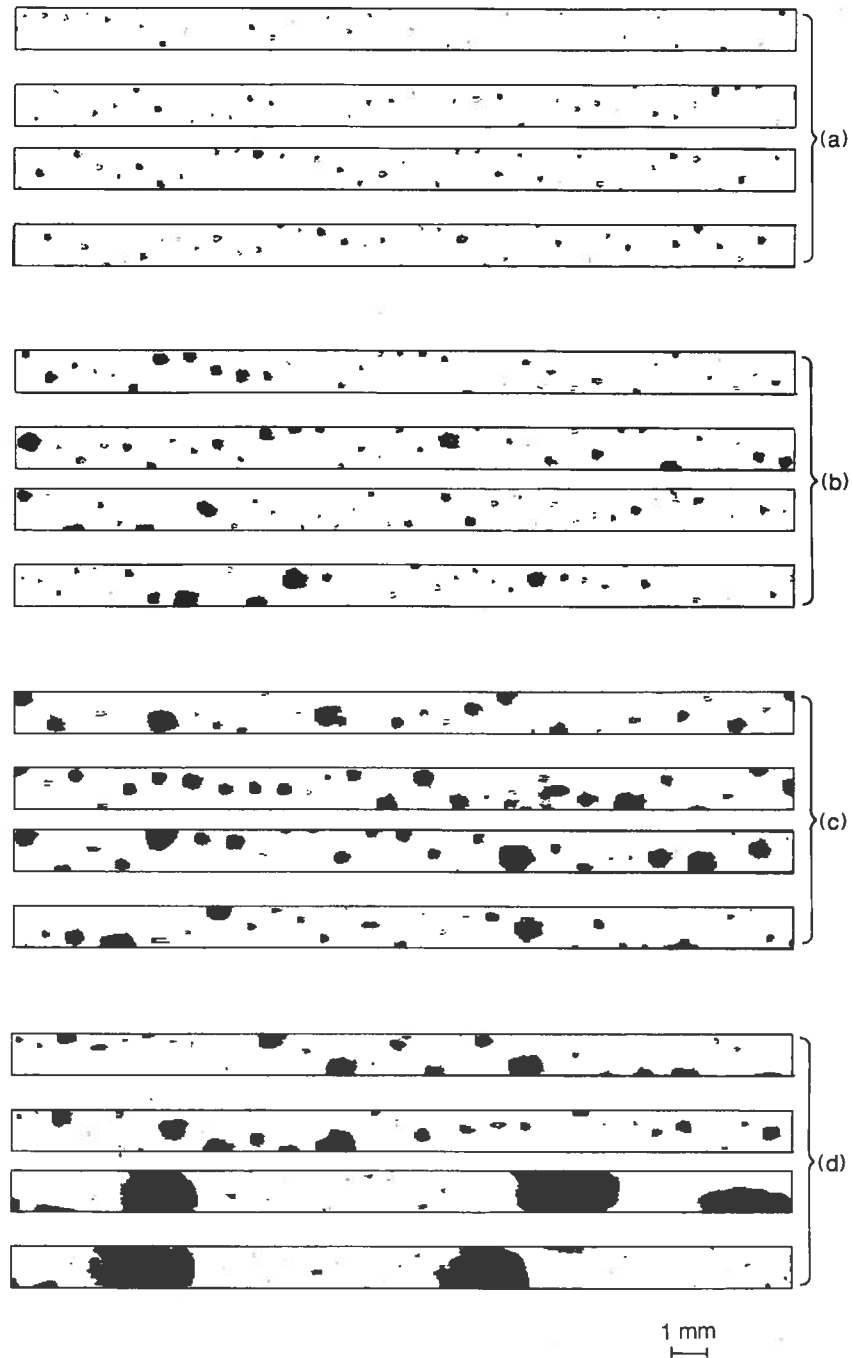


Fig. 11. Examples of particle images from the Citation PMS 2DC probe for each of the ice regions in Figs. 5, 6, 7 and 9. These are labeled (a)–(d), respectively.

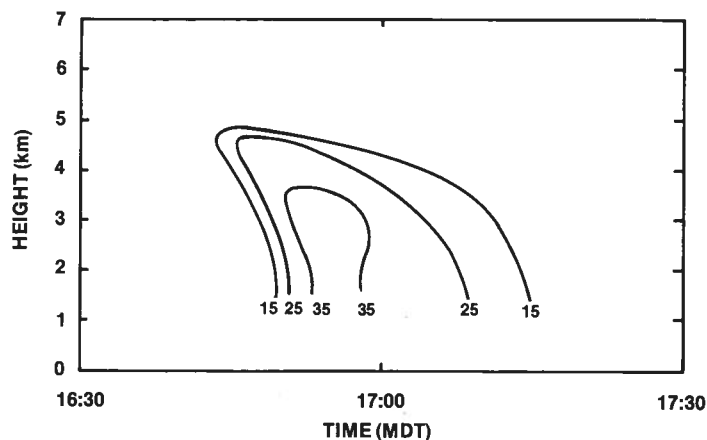


Fig. 12. Height-time plot of local maximum radar reflectivity factors from the CHILL radar data from the 28 June 1987 case. Contours are labelled in dBz.

would be a reasonable first-echo temperature for a cloud with moderate up-drafts seeded with AgI (Miller and Smith, 1986) but is also consistent with the view that the initial ice particles developed at higher levels. The particles observed near the first-echo level at about that time (Fig. 11c) were large enough to produce detectable echoes. The echo persisted for about 30 minutes, reaching an intensity of nearly 40 dBz at low levels and a maximum height of 5.0 km MSL.

DISCUSSION

The results from the 22 June case show that the cloud chamber nucleation rates of DeMott et al. (1983) for the AgI-AgCl aerosol are similar to those which occur in treated natural clouds, provided that the cloud conditions are similar to those in the chamber and that the effects of dilution are accounted for. However, conditions in the natural clouds rapidly change, so it is difficult to match the laboratory conditions for more than brief periods in cloud lifetimes. These findings regarding the time for ice nucleation and growth are also consistent with observations by Kochtubajda (1985), who found that 5–10 min were required to observe the maximum ice crystal production from an AgI-NaIO₃ aerosol (which also acts primarily by contact nucleation). With the SF₆ tracer we are also able to determine the dilution of the aerosol and so estimate the expected particle concentrations. The SF₆ tracer is helpful in determining the origin of the first ice in the cloud, but for most clouds the connection with the ice eventually becomes lost as larger particles develop, due to the effects of particle fallspeed and aggregation.

The results from 28 June show that the material released at cloud base reached and dispersed across the supercooled part of the cloud as intended.

The tracer and accompanying aerosol filled most of the cloud containing supercooled liquid water at the -4°C level within 11 min after the beginning of treatment. The materials were even more fully dispersed across the cloud on subsequent penetrations at higher levels in the cloud.

The 28 June observations also confirm the expectation that, at a given level in a cloud, the early ice concentrations are closely related to the temperature history of the air encountered at that location. For example, at the -7°C level (Fig. 5) the updraft with concentrated tracer (and AgI-AgCl aerosol) had not yet developed measurable ice, while the downdrafts with more dilute tracer had appreciable ice. At the -10°C level (Figs. 6, 7), ice had only begun to develop in the upshear portion of the cloud, where cloud droplets were rising from warmer levels. On the downshear side higher ice concentrations were observed in the downdraft regions, which were bringing air down from lower temperatures.

The observations are consistent with early ice formation in the cloud by the AgI-AgCl aerosol at temperatures low enough for it to produce significant ice particle concentrations. Of course, as with any seeding candidate, some contribution by natural ice-forming processes cannot be excluded. However, the tracer measurements suggest that the natural ice concentrations must have been relatively low. Otherwise, the observed ice concentrations would have exceeded those which would be expected from the AgI treatment alone, and more ice would have appeared in locations separate from the tracer regions. The ice particles were carried downward from their level of formation to the penetration levels first by downdrafts and later, as the particles grew larger, by their settling velocities. At the later stages of graupel development the fall speeds of the large particles would rapidly carry them down to the -3 to -8°C region of the cloud where secondary ice production by riming could occur (e.g. Harris-Hobbs and Cooper, 1987). Ample amounts of large ($>24\ \mu\text{m}$) cloud droplets were available (Fig. 10), so secondary ice production could have been important during the later stages of the cloud.

There is evidence that moderately large cumuli, after seeding with AgI aerosols, develop precipitation by the formation of ice crystals followed by riming to produce graupel (e.g., Gagin and Neuman, 1981; Isaac et al., 1982). However, the cumulus on 28 June was relatively small and similar to the clouds investigated in HIPLEX-1, which was conducted in nearby Miles City, Montana (290 km west of Dickinson). In these clouds the predominant precipitation formation mechanism after glaciogenic (CO_2) seeding was through aggregation (Cooper and Lawson, 1984), not via the formation of graupel as in the 28 June case. A future paper will compare the characteristics of this cloud to those in HIPLEX to discern the reasons for the differences in precipitation formation mechanisms.

These and our earlier studies indicate that the SF_6 tracer, whether directly released into cumuli or carried up from cloud base, mixes completely through

the upper regions of the cloud. As far as the concentrations of ice particles are concerned, the history of the air found at a given location in the cloud may be at least as important as the concentration of ice nuclei present (at least in the early stages of ice development).

Further similar experiments are planned with both SF₆ alone and the mixture of SF₆ and AgI aerosol. The goals of these experiments are to confirm the lack of influence of the treatment aircraft and the release method on ice particle production, to compare the differences in the origin of ice between seeded and natural cumuli and to investigate the transport and dispersion of the tracer under a greater variety of conditions in cumuli.

ACKNOWLEDGMENTS

Support for this research was provided through NOAA as part of the Federal/State Cooperative Program in Weather Modification Research, under Cooperative Agreements NA87RAH07088 and NA866RA8H6058 between NOAA and the North Dakota Atmospheric Resource Board (NDARB). The NDARB administered the work under Contract No. NDARB-UND-NOAA-87 to the University of North Dakota and NDARB-IAS-87-1 to the South Dakota School of Mines and Technology. The T-28 activities were also supported by the National Science Foundation (NSF) under Cooperative Agreement ATM-8620145. We thank the field crews for their contributions; the CHILL radar facility operated by the Illinois State Water Survey with NSF support for supplying the radar data; George Wilkerson, Don Griffith, Diane Odegard, Marcia Politovich and Mike Huston for their assistance; and R. Lynn Rose for his inspiration.

REFERENCES

- Baumgardner, D., Strapp, W. and Dye, J., 1985. Evaluation of the forward scattering spectrometer probe, Part II. Corrections for coincidence and dead-time losses. *J. Atmos. Ocean. Technol.*, 2: 626-632.
- Benner, R.L. and Lamb, B., 1985. A fast response continuous analyzer for halogenated atmospheric tracers. *J. Atmos. Ocean. Technol.*, 2: 582-589.
- Cooper, W.A. and Lawson, R.P., 1984. Physical interpretation of results from the HIPLEX-1 experiment. *J. Clim. Appl. Meteorol.*, 23: 523-540.
- DeMott, P.J., Finnegan, W.G. and Grant, L.O., 1983. An application of chemical kinetic theory and methodology to characterize the ice nucleating properties of aerosols used for weather modification. *J. Clim. Appl. Meteorol.*, 22: 1190-1203.
- Dickerson, R.R., Huffman, G.J., Luke, W.T., Nunnermacker, L.J., Pickering, K.E., Leslie, A.C.D., Linsey, C.G., Slinn, W.G.N., Kelly, T.J., Daum, P.H., Delany, A.C., Greenberg, J.P., Zimmerman, P.R., Boatman, J.F., Ray, J.D. and Stedman, D.H., 1987. Thunderstorms: an important mechanism in the transport of air pollutants. *Science*, 235: 460-465.

- Gagin, A. and Neuman, J., 1981. The second Israeli randomized cloud seeding experiment: evaluation of the results. *J. Appl. Meteorol.*, 20: 1301-1311.
- Greenbut, G.K., 1986. Transport of ozone by cumulus clouds between boundary layer and cloud layers. *J. Geophys. Res.*, 9: 8613-8622.
- Greenhut, G.K., Ching, J.K.S., Pearson, R. and Repoff, R.T., 1984. Transport of ozone by turbulence and clouds in an urban boundary layer. *J. Geophys. Res.*, 89: 4757-4766.
- Harris-Hobbs, R.L. and Cooper, W.A., 1987. Field evidence supporting quantitative predictions of secondary ice production rates. *J. Atmos. Sci.*, 44: 1071-1082.
- Isaac, G.A., Strapp, J.W., Schemenauer, R.S. and MacPherson, J.I., 1982. Summer cumulus cloud seeding experiments near Yellowknife and Thunder Bay, Canada. *J. Appl. Meteorol.*, 21: 1266-1285.
- Johnson, G.N. and Smith, P.L., Jr., 1980. Meteorological instrumentation system on the T-28 thunderstorm research aircraft. *Bull. Am. Meteorol. Soc.*, 61: 972-979.
- Kochtubajda, B., 1985. The evolution of hydrometeor size distributions in seeded Alberta summertime cumulus clouds. 4th WMO Sci. Conf. Weather Modification, WMO/IAMAP Symp., Honolulu, WMO/TD-No. 33, Geneva, I: 77-80.
- Miller, J.R., Jr. and Smith, P.L., 1986. Some characteristics of radar first echoes in the High Plains. *J. Weather Modif.*, 18: 95-101.
- Rangno, A.L. and Hobbs, P.V., 1984. Further observations of the production of ice particles in clouds by aircraft. *J. Clim. Appl. Meteorol.*, 23: 985-987.
- Reinking, R.F., 1985. An overview of the NOAA Federal-State Cooperative Program in weather modification research. 4th WMO Sci. Conf. Weather Modification, WMO/IAMAP Symp., Honolulu, WMO/TD-No. 33, Geneva, II: 643-648.
- Stith, J.L. and Benner, R.L., 1987. Applications of fast response continuous SF₆ analyzers to in situ cloud studies. *J. Atmos. Ocean. Technol.*, 4: 599-619.
- Stith, J.L. and Politovich, M.K., 1989. Observation of the effects of entrainment and mixing on the droplet size spectra in a small cumulus. *J. Atmos. Sci.*, 46: 908-919.
- Stith, J.L., Griffith, D.A., Rose, R.L., Flueck, J.A., Miller, J.R., Jr. and Smith, P.L., 1986. Aircraft observations of transport and diffusion in cumulus clouds. *J. Clim. Appl. Meteorol.*, 25: 1959-1970.